Numerical Modeling of Dynamic Effects in Porous Media Flow

Hans Janssen, PhD **Gregor A. Scheffler, PhD**

ABSTRACT

Moisture is a key determinant when assessing durability and sustainability of buildings and health and comfort of building occupants. The correct design or remediation of built structures thus requires reliable estimation of moisture transfer in porous building materials. A primary concept in any description of porous media moisture transfer is the moisture retention curve. It is generally accepted that process dynamics do not influence such capillary pressure/moisture content relations

The experimental evidence shown in this paper contradicts that assumption, however: simultaneous measurement of local moisture contents and relative humidities during the drying of calcium silicate insulation and aerated autoclaved concrete yields dynamic moisture retention curves deviating from their static counterparts. The measurements moreover show a quick initial drop in local relative humidities, which cannot be reproduced by standard static simulation of the drying process. The simulations result in a similar quick initial drop only if dynamic effects are accounted for.

The further impacts of these findings are large: neglecting the dynamic effects during material property calibration may lead to flawed storage and transport properties, while neglecting dynamic effects in common simulation of moisture transfer may lead to erroneous assessments.

INTRODUCTION

Porous media fluid flow is omnipresent: it takes place at the microscale of cell biology as well as at the macroscale of oil extraction. Similarly in the built environment, porous media flow plays a key role, as it determines the transfer of moisture, and chemicals dissolved therein, in built structures. As such, porous media flow affects the durability and sustainability of built structures: the corrosion of reinforcement bars in concrete due to chloride ingress via pore water is just one example of potential damage. Porous media flow similarly influences the health and comfort of building occupants: excessive interior humidity levels may yield mold formation or depreciate indoor air quality. Often, moisture is the main determinant when assessing the durability and sustainability of built structures or the health and comfort of building occupants.

Thus, for the correct design of novel structures or for the remediation of defective existing ones, dependable estimations of moisture transfer in porous building materials are essential. In recent years, the use of numerical tools for moisture transfer in building materials, building components, and whole buildings has gained a sizeable foothold. Hygrothermal simulation has recently been standardized (*EN Standard 15026-2007*), complemented by a quality assessment methodology (Hagentoft et al. 2004). Amongst others, Gawin et al. (2006) and Nyman et al. (2006) report on simulation models to study the performance and durability of building materials. Finally, various whole-building heat, air, and moisture transfer simulation models were developed recently during the IEA Annex 41 project, Whole Building Heat Air and Moisture Response (Woloszyn and Rode 2008).

A key concept in any description of porous media moisture transfer is the moisture retention curve: the relationship

Hans Janssen *is an associate professor in the Department of Civil Engineering at the Technical University of Denmark, Kgs. Lyngby, Denmark.*
Gregor A. Scheffler *is a researcher at Xella Technologie- und Forschungsgesellschaft, Kloster Lehnin, Germany.*

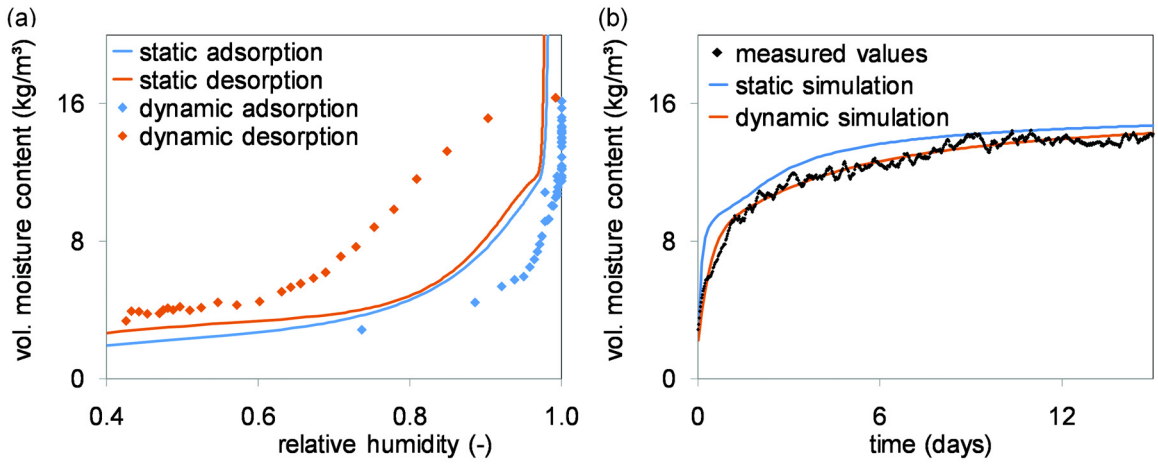

Figure 1 *(A) Static and dynamic isotherms for calcium silicate insulation: dynamic isotherms are obtained from a 33% to 97% RH hygroscopic adsorption and a 97% to 33% RH hygroscopic desorption. (B) Measured and simulated local moisture contents for a 33% to 97% RH hygroscopic adsorption in calcium silicate insulation.*

between capillary pressure and moisture content. It is generally assumed that moisture retention curves determined from static measurements are applicable for transient flow conditions, and vice versa. In other words, it is assumed that the process dynamics do not affect the capillary pressure/moisture content relation; an immediate equilibrium between capillary pressure and moisture content is presumed. Recent evidence suggests, however, that this is not always valid: Hassanizadeh et al. (2002) and Scheffler and Plagge (2009) illustrate that moisture retention curves are affected by the (de)saturation rates of the moisture transfer process concerned (the so-called dynamic effects). Their overall impact on general moisture transfer in porous media is currently debated. These dynamic effects are not limited to two-phase moisture/air displacements in porous media: dynamic effects have equally been observed for oil/water displacements in soil (Porter et al. 2006), and for liquid composite molding (Kim and Daniel 2007).

To provide further insight into the occurrence and influence of dynamic effects for moisture transfer in built structures, this paper centers on numerical modeling of drying experiments. Such drying tests are frequently used for characterization of the moisture permeability, by fitting numerical simulations to measurement data (Carmeliet and Roels 2001; Scheffler 2008; Scheffler and Plagge 2010). An intrinsic deviation between a simulation applying the static theory and a measurement affected by dynamic effects may disturb the reliability of the resultant material properties. As such any simulation using these would also be affected.

The paper is organized as follows. A literature study concisely summarizes past findings on dynamic effects first. Secondly, the main results of the drying measurements are presented, with focus on measured moisture mass integrals, local moisture contents and local relative humidities. The next section introduces the numerical model, and presents the simulation results for the drying experiments. The discussion section analyzes the potential impact of the reported findings, after which conclusions are drawn.

LITERATURE REVIEW

Experimental Evidence of Dynamic Effects

The earliest evidence of dynamic effects in moisture flow in porous media was found for soils (Topp et al. 1967; Smiles et al. 1971). The authors showed that applying a higher desorption rate in outflow experiments (moisture retention measurement procedure, common in soil physics) leads to increased deviations from the static moisture retention curves. While these authors restricted their measurements to sandy soils with narrow pore-size distribution, and to drainage processes in the high-moisture-content range, Wanna-Etyem (1982) corroborated dynamic effects in fine- and coarse-textured soils and for both imbibition and drainage processes. To conclude Hassanizadeh et al. (2002) reanalyzed various moisture retention curves measured by other authors, revealing widespread occurrence of dynamic effects.

In building physics, new evidence of dynamic effects has been reported by Plagge et al. (2006) and Scheffler and Plagge (2009). By systematic simultaneous measurement of local relative humidity and moisture content, they obtained dynamic sorption isotherms deviating from independently measured static isotherms: the first evidence that dynamic effects also occur in the hygroscopic range. Figure 1A compares the static isotherm of calcium silicate insulation with dynamic isotherms obtained from a 33% to 97% RH adsorption and 97% to 33% RH desorption. Moreover, comparison of experiments and simulations indicated significant deviations (Scheffler 2008). All observed trends corresponded with predictions based on dynamic-effects theory.

General observations show that dynamic effects yield lower moisture retention for absorption processes (a lower moisture content in comparison to the static curve at the same capillary pressure), while higher retention is observed for desorption processes. Moreover, dynamic effects are shown to be proportional to the (de)saturation rate and inversely proportional to the permeability. This renders building materials, with their low permeability in comparison to soils, particularly susceptible to dynamic effects. The global impact of dynamic effects on general moisture transfer in porous media is, however, still debated.

Functional Description of Dynamic Effects

The primary concept of dynamic effects is the invalidity of the immediate equilibrium between capillary pressure and moisture content, generally accepted in porous media flow. This finite relaxation rate of moisture contents in response to capillary pressure changes was reproduced by Dahle et al. (2005) with a bundle-of-tubes pore scale model. By explicit inclusion of interfaces and interfacial properties in the macroscale theory of two-phase flow, Hassanizadeh et al. (2002) arrived at a more general definition of capillary pressure, permitting coexistences of capillary pressure and moisture content deviating from the common static moisture retention curve. A linear relation is assumed:

$$p_c^{dyn}(S) - p_c^{stat}(S) = \tau \frac{\partial S}{\partial t} \quad (1)$$

where

p_c^{dyn} = dynamic capillary pressure, Pa
p_c^{stat} = static capillary pressure, Pa
S = saturation, dimensionless
τ = material coefficient, kg/(m·s)
t = time, s

Equation 1 states that, under steady-state conditions with no change in saturation, the actual dynamic capillary pressures are equal to the static capillary pressures, and hence in equilibrium with the moisture contents. During a transient adsorption process, however, dynamic capillary pressures can be higher than their related static counterpart, and vice versa for desorption. The extent of the deviations depends on the material coefficient τ, thus rendering it a measure for the pore water relaxation times.

Numerical Simulation of Dynamic Effects

Hassanizadeh et al. (2002) used Equation 1 for numerical simulation of capillary water uptake in soils with consideration of dynamic effects. The results demonstrated that the infiltration was severely reduced, indicating that dynamic effects may substantially affect moisture flow in soils. Since their simulation was limited to just one loading condition and one soil, no general conclusions on the potential impact of dynamic effects on moisture transfer in building materials, building components or whole buildings can be drawn.

Janssen and Scheffler (2009) applied Equation 1 for numerical simulations of hygroscopic adsorption, capillary absorption, and isothermal drying. The validity of the numerical model was verified by comparison with experimental results for hygroscopic adsorption. Local moisture contents and relative humidities were determined during a 33% RH to 97% RH hygroscopic adsorption into 10 cm of calcium silicate insulation. The measured moisture content at 1 cm from the adsorption boundary condition, a static simulation (excluding dynamic effects), and a dynamic simulation (including dynamic effects) are compared in Figure 1B. It is obvious that the static moisture transfer theory does not suffice to simulate hygroscopic adsorption, and hence that dynamic effects need to be considered to correctly model this very common process. Janssen and Scheffler (2009) continued with dynamic effect simulations of capillary absorption and isothermal drying processes, which established that dynamic effects have a potentially significant impact and should thus not be disregarded in the description of moisture transfer in porous media.

EXPERIMENTAL RESULTS

Drying Experiments

Drying experiments were executed on a 80 mm (3.15 in.) high calcium silicate insulation (CaSi) sample and a 40 mm (1.57 in.) high aerated autoclaved concrete (AAC) sample. The CaSi density was 280 kg/m^3, effective porosity 91%, and capillary moisture content 880 kg/m^3, and the AAC density was 400 kg/m^3, effective porosity 70%, and capillary moisture content 275 kg/m^3. The drying experiments made use of a specific drying device that drove interior air over the bottom drying surface of the sample by means of small fans. Prior to drying, the CaSi and AAC samples were capillarily saturated with a free water uptake experiment.

During the drying, moisture content distributions in the sample were determined with x-ray projection for the whole 80 mm (3.15 in.) of the CaSi sample and for the bottom 23.6 mm (0.93 in.) of the AAC sample. Relative humidities in the samples were determined with relative humidity sensors and thermocouple psychrometers at two locations: at 40 mm and 60 mm (1.57 in. and 2.36 in.) above the drying surface for CaSi, and at 10 mm and 17 mm (0.39 in. and 0.67 in.) above the bottom drying surface for AAC. An illustration of the CaSi drying setup in the x-ray measurement chamber is found in Figure 2.

Additional sensors monitored the temperature and relative humidity of the interior air. The drying experiments covered respectively 16 and 6.7 days for CaSi and AAC, at the end of which the drying processes were well into their second drying phase. Further continuation until equilibrium with the environment was deemed unnecessary, as the minute desaturation rates nullify the potential impact of dynamic effects.

The accuracy of the x-ray measurements was quantified with a method similar to that of Roels and Carmeliet (2006): a resolution well below 1 kg/m^3 was obtained, sufficient for the

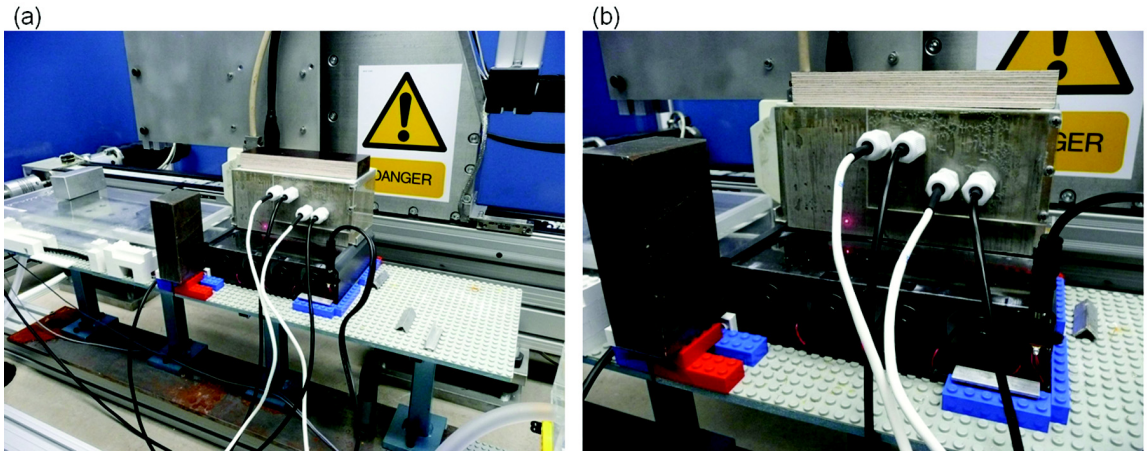

Figure 2 *Illustration of measurement setup for controlled drying experiments in the x-ray chamber. Little fans were used to drive air over the drying surface. The four connections are two relative humidity sensors and two thermocouple psychrometers. In the setup shown, the calcium silicate insulation sample is featured.*

moisture contents targeted during the drying experiments. The relative humidity sensors were new and recently calibrated by the producer. Their stated absolute accuracy was ±0.8%. Their performance was verified above oversaturated salt solutions (RHs 11.3% to 97.6%), and judged excellent. The thermocouple psychrometers were calibrated above unsaturated salt solutions (RHs 96.7% to 99.98%), demonstrating an absolute accuracy of ±0.1% or better. Such accuracies are sufficient for the relative humidities targeted during the drying experiments.

Measurement Results

The measured moisture content distributions were transformed to moisture mass integrals for the measured section of the samples and to local moisture contents for the locations at which relative humidities are obtained. A graphical illustration for the CaSi sample is given in Figure 3.

The local relative humidities were measured in two ways: a thermocouple psychrometer for the range above 96% RH, and a relative humidity sensor for the range below 98% RH. The final local relative humidities were obtained as a combination of the two signals. In the early parts of the measurement, the higher relative humidities were taken from the psychrometers, while the lower relative humidities during the later parts were taken from the humidity sensors. The obtained evolutions of local relative humidities with time are also shown in Figure 3. It can be seen that the two sensor results overlap between 96% RH and 98% RH, confirming the reliability of the measurements.

Simultaneous values of local relative humidities and moisture contents can be combined into dynamic moisture retention curves, which are compared to the static desorption moisture retention curves for CaSi and AAC in Figure 4. It is clear that the dynamic retention curves do not correspond to the static desorption curves, a primary indication of dynamic effects. It can moreover be noted that the deviations are largest for the lower locations, closest to the drying surface (40 mm [1.57 in.] for CaSi, 10 mm [0.39 in.] for AAC): the desaturation speed is largest at these locations, hence maximizing the dynamic effects. Combination of the differences between dynamic and static desorption curves with the desaturation rates leads to the dynamic-effects material parameter τ, also shown in Figure 4. The general order of magnitude for the drying tests examined is 10^{11} kg/(m·s) to 10^{14} kg/(m·s).

Hassanizadeh et al. (2002) obtained 10^{3} kg/(m·s) to 10^{7} kg/(m·s) for soil inflow and outflow experiments (thus in the high moisture content range). Janssen and Scheffler (2009) came to 10^{14} kg/(m·s) to 10^{15} kg/(m·s) from hygroscopic adsorption measurements (thus in the low moisture content range). It is clear that τ depends on the moisture content. Whether τ similarly depends on the nature of the moisture transfer process itself cannot be decided from the current data. For the modeling, τ is assumed constant at 10^{12} kg/(m·s) for CaSi, while a variation is assumed for AAC: both approximations are shown in Figure 4.

NUMERICAL RESULTS

Numerical Model

All simulation results in this paper are obtained from an enhanced version of a numerical simulation model for building component heat and moisture transfer (Janssen et al. 2007), solving the moisture transfer equation with a finite-element-based spatial discretization and a full-implicit temporal discretisation. If dynamic effects are assumed insignificant, Equation 2 describes one-dimensional isothermal transfer of moisture. Equation 2 applies static moisture retention curves to relate capillary pressures to moisture contents.

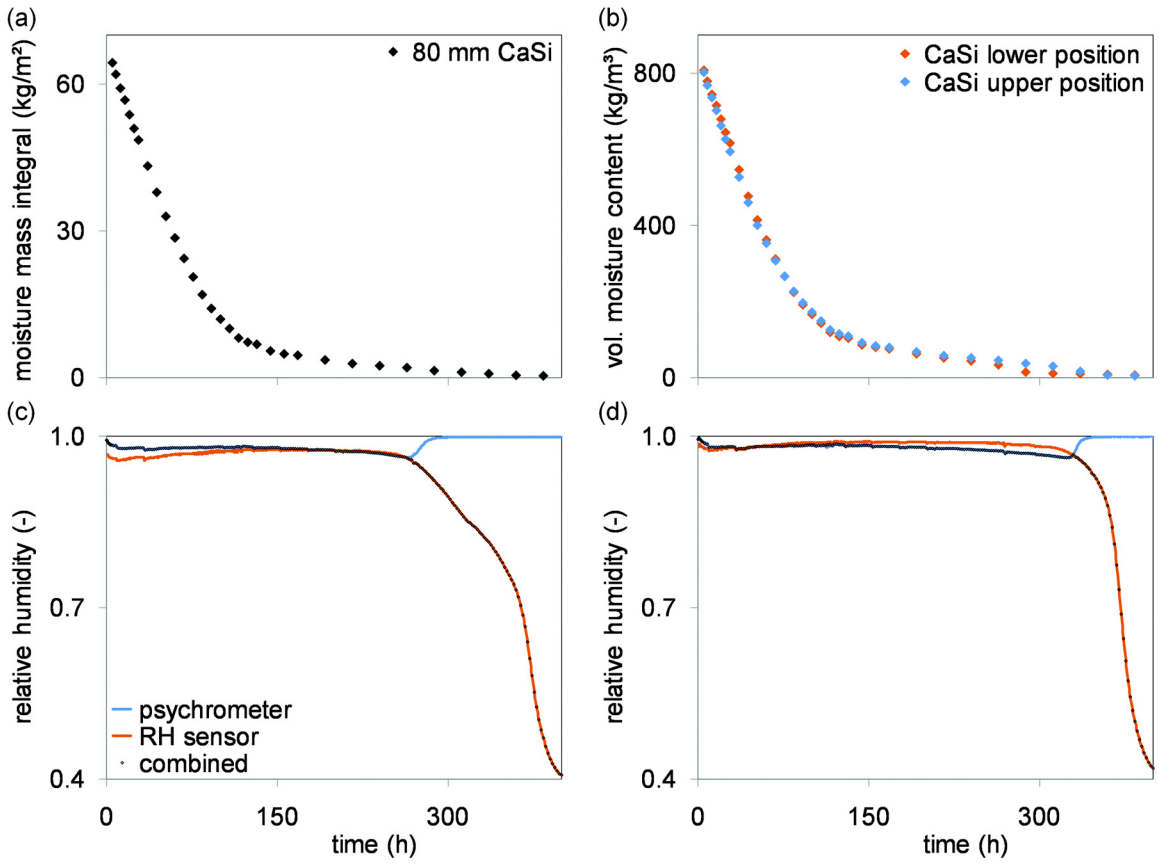

Figure 3 *Measurement results for controlled drying of CaSi; (A) moisture mass integral, (B) local moisture contents, (C) local relative humidity for lower location, (D) local relative humidity for upper location.*

$$\frac{\partial w}{\partial t} = -\frac{\partial}{\partial x}\left[K\frac{\partial p_c^{stat}}{\partial x}\right] \qquad (2)$$

where

w = moisture content, kg/m^3

x = space coordinate, m

K = moisture permeability, s

When dynamic effects are considered significant, Equation 3 describes one-dimensional isothermal transfer of moisture. Equation 3 uses dynamic moisture retention curves, defined by Equation 1, to relate capillary pressures to moisture contents.

$$\frac{\partial w}{\partial t} = -\frac{\partial}{\partial x}\left[K\frac{\partial p_c^{dyn}}{\partial x}\right] \qquad (3)$$

Equation 1 defines the main complexity of numerically solving Equation 3: the variability of the dynamic moisture retention curve in time and space, as local moisture retention is affected by the local (de)saturation rate. A straightforward option to solve Equation 3 is to iteratively alternate with Equation 1. The dynamic capillary pressures from Equation 3 are transformed to related static pressures with Equation 1. These are then used to calculate moisture contents, capacities, and permeabilities for the following iteration. As the local (de)saturation rate may change with each iteration, so does the local moisture retention curve, yielding instability. Hassanizadeh et al. (2002) suggested directly inserting Equation 1 into Equation 3:

$$\begin{aligned}\frac{\partial w}{\partial t} &= -\frac{\partial}{\partial x}\left[K\frac{\partial}{\partial x}\left(p_c^{stat} + \tau\frac{\partial S}{\partial t}\right)\right] \\ &= -\frac{\partial}{\partial x}\left[K\frac{\partial}{\partial x}\left(p_c^{stat} + \alpha\frac{\partial w}{\partial t}\right)\right] \qquad \alpha = \frac{\tau}{\rho_l \varepsilon}\end{aligned} \qquad (4)$$

where

α = material coefficient, m^2/s

ρ_l = density of water, kg/m^3

ε = material porosity, dimensionless

The parameter α is equivalent to τ, but now with the (de)saturation rates expressed as moisture content changes. In Equation 4, the last term on the right-hand side is rewritten in function of the static capillary pressures, with the mass-conservative scheme (Janssen et al. 2007). The final Equation 4 results in a far more stable numerical problem.

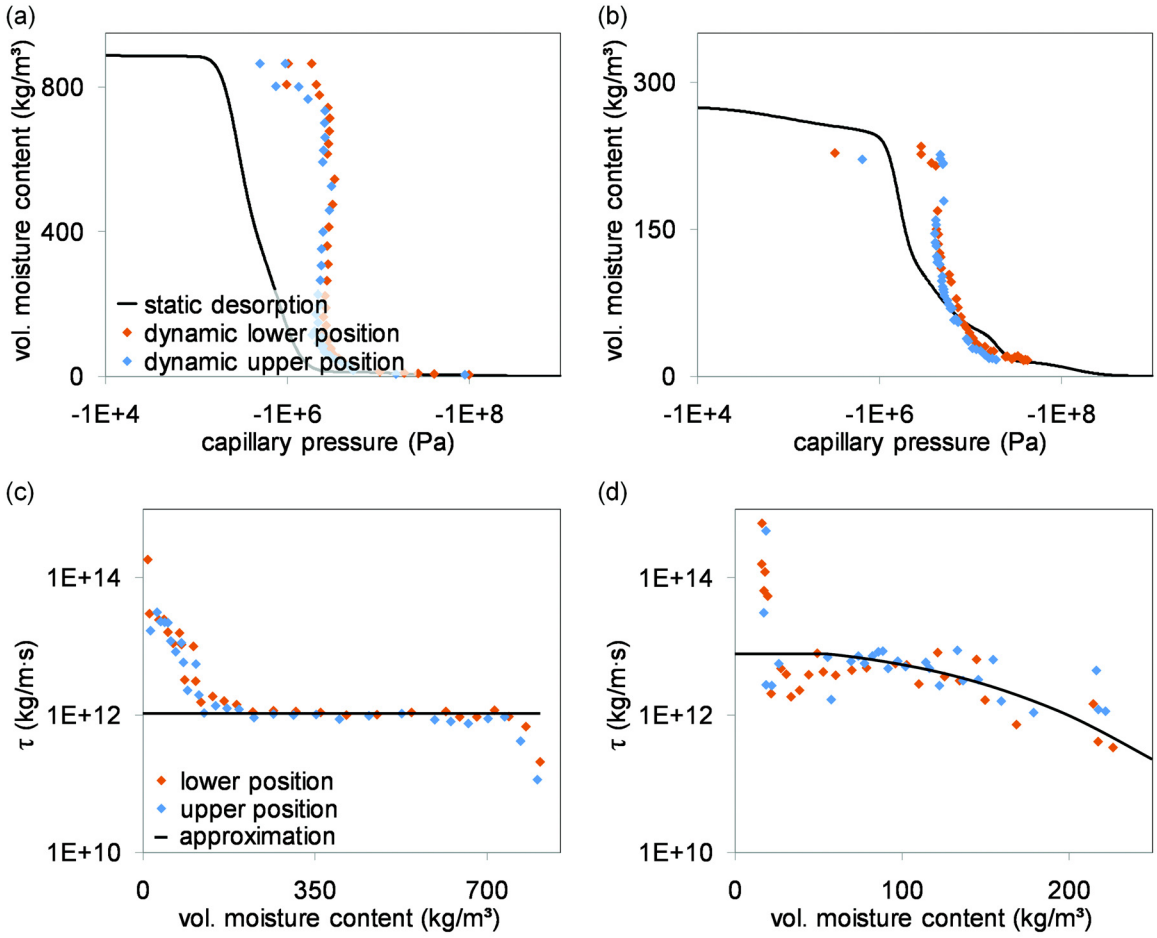

Figure 4 *Static and dynamic moisture retention curves (A) for CaSi, (B) for AAC. Measurement and approximation of* τ*, (C) for CaSi, and (D) for AAC.*

While temperature variations in the interior air and latent heat transfer at the drying surface essentially result in nonisothermal drying, it has been assumed here that an isothermal drying simulation suffices to reliably calculate the process. The interior air was at 22.5°C (72.5°F) and 37% RH during the CaSi drying and the surface moisture transfer coefficient was assumed 1.0×10^{-7} kg/(m^2·s·Pa). These conditions are 22.5°C (72.5°F), 40% RH, and 1.1×10^{-7} kg/(m^2·s·Pa) for AAC drying.

CaSi Drying Results

Static Simulation. At first a static (i.e., applying static moisture retention curves) simulation was performed. The desorption moisture retention curve and moisture permeability used were determined previously, based on a hygric material model (Scheffler and Plagge 2010). It is crucial to note that this model does not only consider measured values for moisture retention and transport, but also includes a calibration to capillary absorption and controlled drying experiments (for which static simulations were used).

The static simulation results for the CaSi drying are shown in Figure 5 as moisture mass integral and as local moisture contents and relative humidities. Comparison with measured values indicates that the moisture mass integral and the local moisture contents were approximated reasonably well. Local relative humidities, on the other hand, were overestimated by the simulations: the measurements roughly yielded 98% RH, while the simulations resulted in values of around 99.8% RH. This is a key indication of dynamic effects: higher water retention during the desaturation process. During drying, the relative humidities drop, in response to the drying boundary condition. The moisture contents follow that drop, but the moisture mass that needs to be dried out via the boundary forms the inertia, controlling the drop in relative humidities. If no dynamic effects were at play, the relative humidities would remain high as long as the moisture contents traveled down along the steep drop in the moisture retention curve (see Figure 4). The simulated 99.8% RH indeed corresponds to a capillary pressure of 3×10^5 Pa, representative for the main drop in the CaSi retention curve. Dynamic effects would, however, enable a faster decrease in relative humidities, as

they allow higher water retention. Dynamic effects thus permit the relative humidities to respond more quickly to the drying boundary condition, as more moisture can be retained at lower relative humidities (see Figure 4).

Dynamic Simulation. This principle is illustrated by the result of dynamic simulations. The first dynamic simulation uses the original moisture permeability, initially calibrated to controlled drying experiments with a static simulation model. Figure 5 shows that the prediction of local relative humidities immediately improves: including dynamic effects permits reproducing the initial drop in RH to around 98% RH, which is impossible with a static simulation.

After around 90 hours, however, the simulated RH jumps up, in contrast to the stable measurement. This originates from the sudden decrease in the simulated desaturation rate: just after 90 hours, the second drying phase starts quite abruptly, lowering the desaturation rate and thus the impact of dynamic effects. The measurements indicate a slower transition towards the second drying phase, yielding a more stable RH decrease. Comparison of the simulated and measured moisture mass integral and local moisture contents, however, reveals a deficit of the original calibration of the moisture permeability (Scheffler 2008; Scheffler and Plagge 2010): when newly combined with dynamic effects, the length of the first drying phase is overestimated.

The same observation was made by Janssen and Scheffler (2009): dynamic effects enhance moisture retention in a desaturation process. This enhanced moisture retention gives higher permeabilities globally during the drying process; these in turn facilitate an interior redistribution of moisture to the drying surface and thus lengthen the first drying phase. In conclusion, the moisture permeability is to be recalibrated, with consideration for dynamic effects. This generally results in lower permeabilities, an issue discussed in more detail later on in the paper.

The newly simulated moisture mass integral and local moisture contents in Figure 6 indicate that a better calibration of the moisture permeability is required still. For the analysis here, however, the current results are assumed satisfactory. The simulation of local relative humidities suffers from the same defect as before: at around 80 hours, when the second drying phase begins, the simulated RH jumps up while the measurements do not. The phenomenon is again attributable to the abrupt start of the second drying phase in the simulation, lowering the desaturation rates and thus the impact of dynamic effects. This should not be marked as a flaw in the dynamic-effects theory, however, but as a motivation to further improve the calibration of the moisture permeability. Moreover, τ has been assumed constant at 10^{12} kg/(m·s), which becomes questionable for the low moisture contents observed at this stage in the drying process.

AAC Drying Results

Similar observations can be made for the AAC drying. The results from static and dynamic simulations are compiled in Figure 7. As before, static simulation yields good approximations of the moisture mass integral and the local moisture contents, and the simulated local relative humidities are significantly above their measured counterparts. When dynamic effects are included, lower local relative humidities are obtained. The agreements with the measured values for moisture mass integral and local moisture contents are, however, appreciably worse. This is a consequence of the lower quality of the permeability calibration and its impact on the prediction of local moisture contents. The deviations between simulated and measured local moisture contents disturb the calculated desaturation rates, which in turn spoil the dynamic effects and their impact on local relative humidities. The dynamically simulated local relative humidities furthermore undershoot the measured values at the very start of the drying process. This results from a too-high τ value at high moisture contents. The current experimental data do though not allow a more accurate estimation of this parameter.

DISCUSSION

General Findings

The measurement of local moisture contents and relative humidities over time during the drying of CaSi and AAC allowed arriving at dynamic moisture retention curves for both materials. Comparison with their static desorption retention curves showed clear deviations, a primary indication for the occurrence of dynamic effects during the drying process. This is the first time such observation has been reported for this type of process.

The simulations with a static moisture transfer model (i.e., applying static moisture retention curves to relate moisture contents and capillary pressures) allowed attaining acceptable approximations of the moisture mass integrals and the local moisture contents. For the local relative humidities, however, it was observed that the simulations did not reproduce the initial RH drop seen in the measurements. In the measurements, the RHs immediately drop to around 98% RH (CaSi) and 97% RH (AAC), while the simulations resulted in 99.8% RH (CaSi) and 98.7% RH (AAC). Only if dynamic effects are accounted for in the simulation can the quick initial RH drop be reproduced.

It must be noted that quality of the dynamic simulations can still be improved by better calibration of the moisture permeabilities. For now, however, the current outcomes are deemed satisfactory as they conceptually support the occurrence of dynamic effects during the drying process.

Further Impacts

It has been noted earlier that the moisture permeabilities required recalibration when dynamic effects were included in the simulation. This is a logical consequence of the original calibration (Scheffler 2008; Scheffler and Plagge 2010) applying static simulation for a process that is affected by dynamic effects. The moisture retention curve is strongly based on

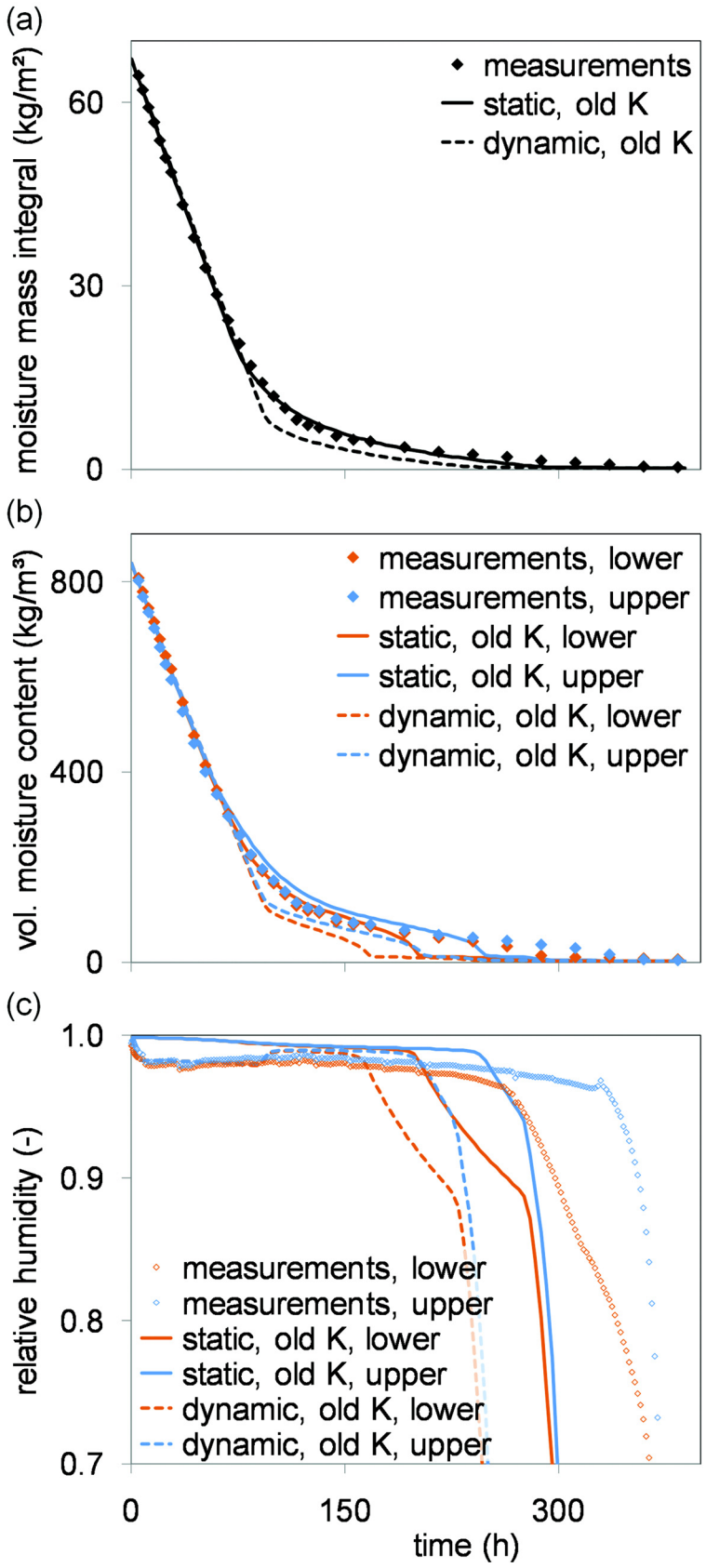

Figure 5 *Measurements and static and dynamic simulations for drying of CaSi: (A) moisture mass integral, (b) local moisture contents, and (C) local relative humidities. Both simulations use statically calibrated permeabilities.*

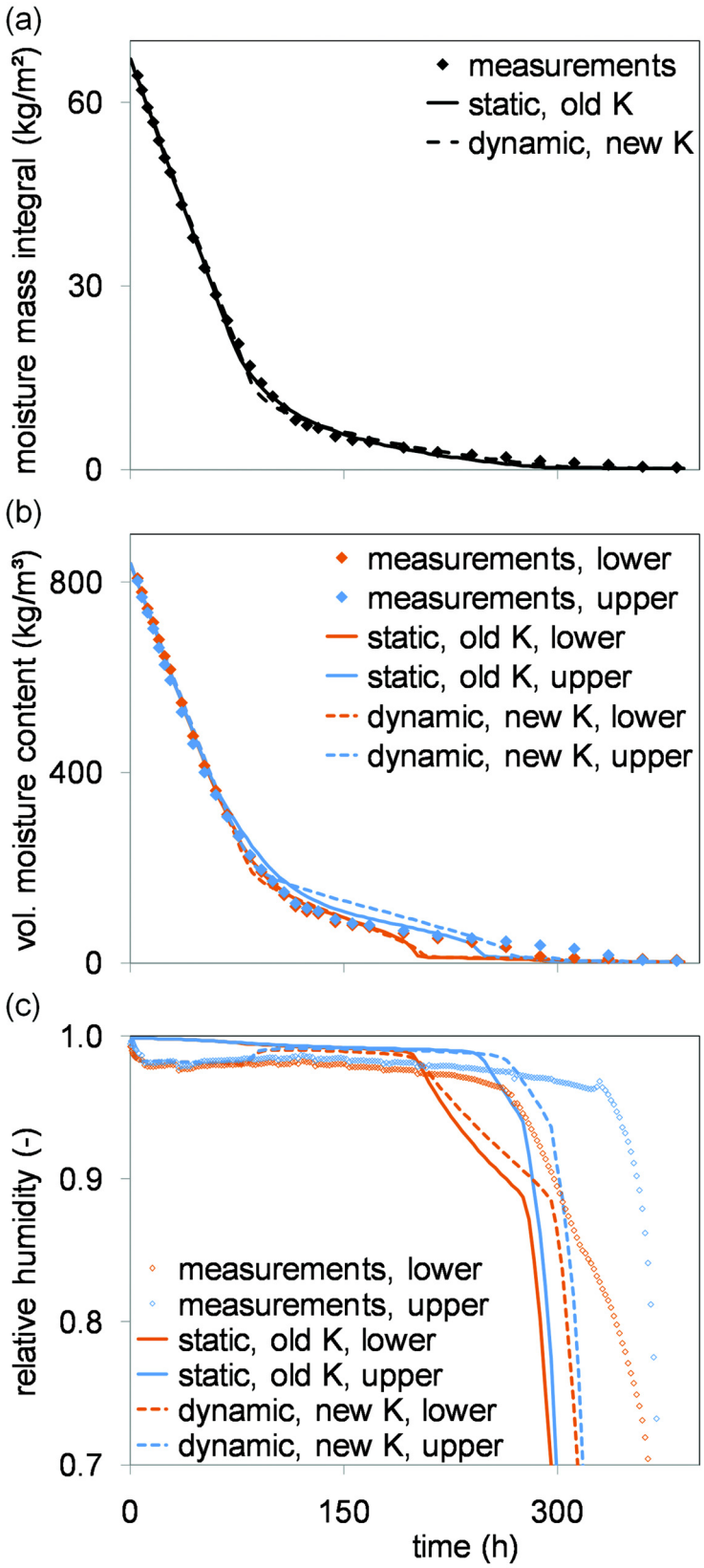

Figure 6 *Measurements and static and dynamic simulations for drying of CaSi: (A) moisture mass integral, (B) local moisture contents, and (C) local relative humidities. The static simulation uses statically calibrated permeabilities; the dynamic simulation uses dynamically calibrated permeabilities.*

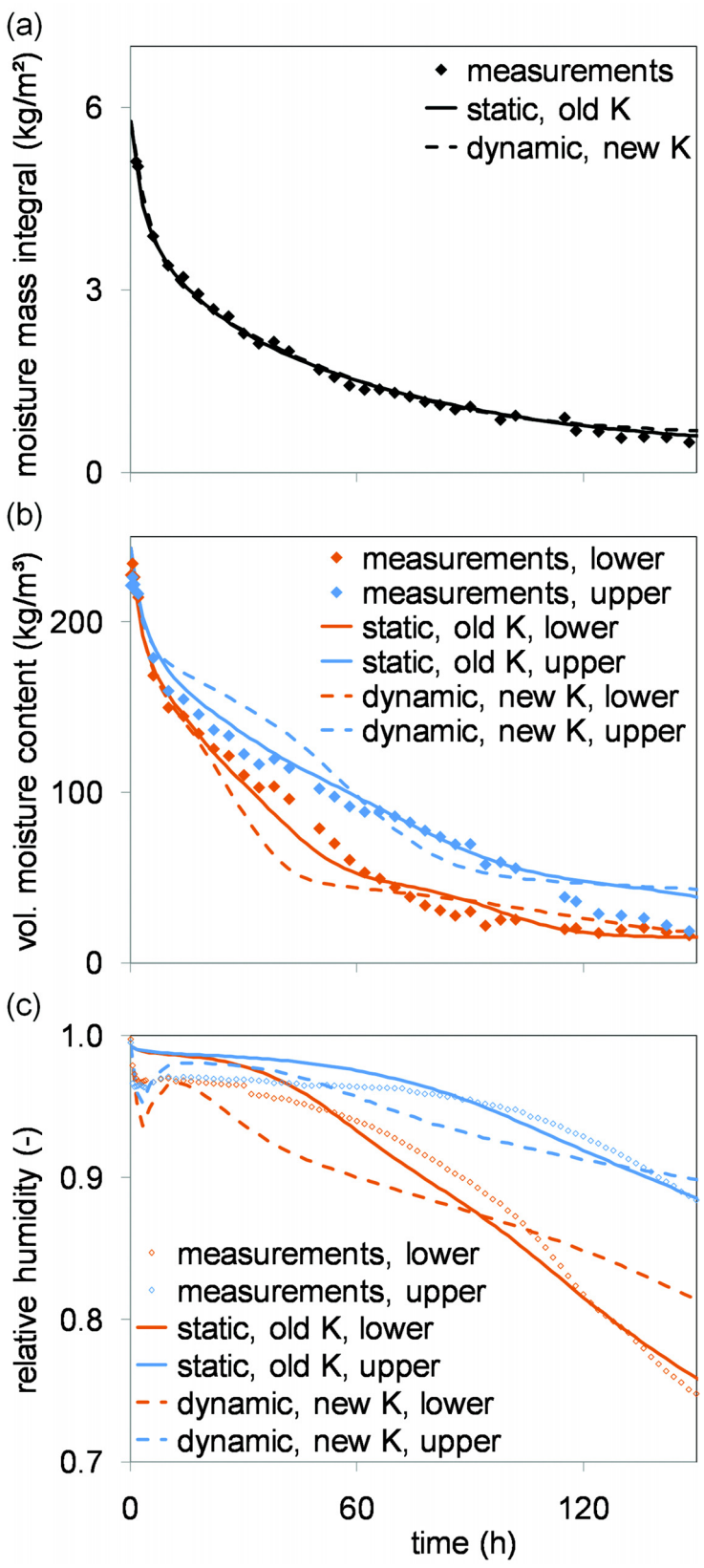

Figure 7 *Measurements and static and dynamic simulations for the drying of AAC: (A) moisture mass integral, (B) local moisture contents, and (C) local relative humidities. The static simulation uses statically calibrated permeabilities; the dynamic simulation uses dynamically calibrated permeabilities.*

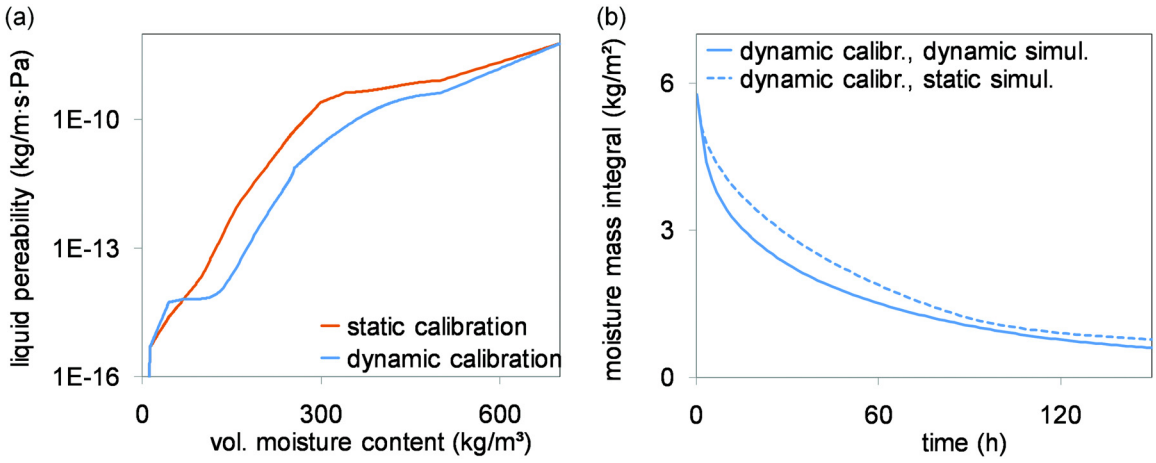

Figure 8 *(A) Comparison of statically and dynamically calibrated permeabilities for AAC, and (B) comparison of static and dynamic simulations (both using dynamically calibrated permeabilities) of drying of AAC.*

measured values, obtained from static experiments, and therefore forms the stable part of the calibration. Measurement of moisture permeabilities is far more difficult, though, and their relation to moisture content is the flexible part of the calibration. This implies that any calibration with static simulations assimilates dynamic effects, physically affecting moisture retention only, by modifying the permeabilities. Calibration with static simulation thus ultimately leads to erroneous permeabilities if dynamic effects are at play. This is illustrated in Figure 8, which compares moisture permeabilities obtained from calibrations with static and dynamic simulations: the static calibration leads to permeabilities surpassing those of the dynamic calibration. Note, however, that the permeabilities resulting from dynamic calibration are to be considered as examples only: the calibration is not of high quality, and is furthermore only based on the newly measured moisture mass integrals during drying. Any influence of the new calibration on the capillary absorption behavior has been neglected.

The reverse is also true, though: application of a static simulation model to judge moisture transfer processes influenced by dynamic effects will equally lead to erroneous estimates. For example, for the AAC drying, application of the dynamically calibrated moisture permeabilities in a static model underestimates the speed of drying. This is illustrated in Figure 8, which compares the measured data to a static simulation and a dynamic simulation both using the dynamically calibrated permeability.

CONCLUSION

In this study, the occurrence of dynamic effects during drying of building materials has been investigated, both experimentally and numerically, by examinations of the controlled drying of calcium silicate insulation and aerated autoclaved concrete samples. In the measurements, moisture content distributions were determined via x-ray projection. Local relative humidities were monitored at two locations, by means of relative humidity sensors and thermocouple psychrometers. For the simulations, a functional description of dynamic moisture retention curves was implemented into a simulation model for moisture transfer in porous media.

The measurement of local moisture contents and relative humidities over time during the drying of CaSi and AAC allowed derivation of dynamic moisture retention curves for both materials. Comparison with their static desorption retention curves showed clear deviations, a primary indication for the occurrence of dynamic effects during the drying process. This is the first time such observation has been reported for this type of process.

The simulations indicated that the quick initial drop in local relative humidities observed in the measurements could not be reproduced with normal static simulation. Only if dynamic effects were considered could such quick initial RH drops be captured numerically. While the dynamic simulation results are certainly improvable (by enhanced calibration of the moisture permeabilities), they conceptually corroborate the occurrence of dynamic effects during the drying processes.

The further implications of these observations were examined, and it was shown that neglecting dynamic effects during material property calibration may result in flawed storage and transport properties, while neglecting dynamic effects in common simulations of moisture transfer may lead to erroneous assessments.

All in all, the findings indicate that the currently generally accepted static moisture transfer theory is incomplete and should be corrected for the widespread occurrence of dynamic effects. To this end, further experimental and numerical work is required. Extensive measurements are required to further corroborate dynamic effects for capillary absorption processes and to determine the relevant τ factors. Comprehensive simulations are required to assess the potential impact of dynamic effects in procedures for material property determination and

for general hygrothermal response estimation. Moreover, attention should be paid to improved independent determination of moisture permeabilities in order to confirm the current calibration techniques in hygric material modeling.

NOMENCLATURE

K = moisture permeability, s
p_c = capillary pressure, Pa
S = saturation, dimensionless
t = time, s
w = moisture content, kg/m^3
x = space coordinate, m
α = material coefficient, m^2/s
ε = material porosity, dimensionless
ρ_l = density of water, kg/m^3
τ = material coefficient, kg/(m·s)

Superscripts

dyn = dynamic
stat = static

REFERENCES

Carmeliet, J. and S. Roels. 2001. Determination of the isothermal moisture transport properties of porous building materials. *Journal of Thermal Envelope and Building Science* 24:183–210.

Dahle, H.K., M.A. Celia, and S.M. Hassanizadeh. 2005. Bundle-of-tubes model for calculating dynamic effects in the capillary pressure–saturation relationship. *Transport in Porous Media* 58:5–22.

EN. 2007. *EN Standard 15026, Hygrothermal performance of building components and building elements—Assessment of moisture transfer by numerical simulation*. European Committee for Standardization.

Gawin, D., F. Pesavento, and B.A. Schrefler. 2006. Hygro-thermo-chemo-mechanical modelling of concrete at early ages and beyond. Part I: Hydration and hygrothermal phenomena. *International Journal for Numerical Methods in Engineering* 67:299–331.

Hagentoft, C.-.E., A.S. Kalagasidis, B. Adl-Zarrabi, S. Roels, J. Carmeliet, H. Hens, J. Grunewald, M. Funk, R. Becker, D. Shamir, O. Adan, H. Brocken, K. Kumaran, and R. Djebbar. 2004. Assessment method of numerical prediction models for combined heat, air and moisture transfer in building components: Benchmarks for one-dimensional cases. *Journal of Thermal Envelope and Building Science* 27:327–352.

Hassanizadeh, S.M., M.A. Celia, and H.K. Dahle. 2002. Dynamic effects in the capillary pressure–saturation relationship and its impacts on unsaturated flow. *Vadose Zone Journal* 1:38–57.

Janssen, H. and G.A. Scheffler. 2009. Dynamic effects in porous media flow: Exploratory modelling. *Proceedings of 4th International Building Physics Conference*, Istanbul Technical University.

Janssen, H., B. Blocken, and J. Carmeliet. 2007. Conservative modelling of the moisture and heat transfer in building components under atmospheric excitation. *International Journal of Heat and Mass Transfer* 50:1128–40

Kim, S.K. and I.M. Daniel. 2007. Observation of permeability dependence on flow rate and implications for liquid composite molding. *Journal of Composite Materials* 41:837–49.

Nyman, U., P.J. Gustafsson, B. Johannesson, and R. Hägglund. 2006. A numerical method for the evaluation of non-linear transient moisture flow in cellulosic materials. *International Journal for Numerical Methods in Engineering* 66:1859–83.

Plagge, R., G. Scheffler, J. Grunewald, and M. Funk. 2006. On the hysteresis in moisture storage and conductivity measured by the instantaneous profile method. *Journal of Building Physics* 29:247–59.

Porter, M.L., M.G. Schaap, and D. Wildenschild. 2006. Capillary pressure–saturation curves: Toward simulating dynamic effects with the lattice-Boltzmann method. *Proceedings of Computational Methods in Water Resources XVI*, Technical University of Denmark.

Roels, S. and J. Carmeliet. 2006. Analysis of moisture flow in porous materials using microfocus x-ray radiography. *International Journal of Heat and Mass Transfer* 49:4762–72.

Scheffler, G.A. 2008. *Validation of hygrothermal material modelling under consideration of the hysteresis of moisture storage*. Doctoral thesis, Dresden University of Technology, Dresden.

Scheffler, G.A. and R. Plagge. 2009. Evidence on dynamic effects in the water content—Water potential relation of building materials. *Proceedings of 4th International Building Physics Conference*, Istanbul Technical University.

Scheffler, G.A. and R. Plagge. 2010. A whole range hygric material model: Modelling liquid and vapour transport properties in porous media. *International Journal of Heat and Mass Transfer* 53:286–96

Smiles, D.E., G. Vauchaud, and M. Vauclin. 1971. A test of the uniqueness of soil moisture characteristic during transient, non-hysteretic flow of water in a rigid soil. *Soil Science Society of America Proceedings* 35:534–39.

Topp, G.C., A. Klute, and D.B. Peters. 1967. Comparison of water content-pressure head data obtained by equilibrium, steady-state, and unsteady-state methods. *Soil Science Society of America Proceedings* 31:312–14.

Wanna-Etyem, C. 1982. *Static and dynamic water content—Pressure head relations of porous media*. Doctoral thesis, Colorado State University, Fort Collins, CO.

Woloszyn, M. and C. Rode. 2008. Tools for performance simulation of heat, air and moisture conditions of whole buildings. *Building Simulation* 1:5–24.